Chapter 4

Raman spectroscopic study of ancient South African domestic clay pottery

Available online at www.sciencedirect.com
ScienceDirect
Spectrochimica Acta Part A 66 (2007) 135–142
SPECTROCHIMICA ACTA PART A
www.elsevier.com/locate/saa

Raman spectroscopic study of ancient South African domestic clay pottery

M.A. Legodi, D. de Waal *

Department Of Chemistry University of Pretoria, Pretoria 0002, South Africa

Received 14 October 2005; accepted 3 February 2006

Abstract

The technique of Raman spectroscopy was used to examine the composition of ancient African domestic clay pottery of South African origin. One sample from each of four archaeological sites including Rooiwal, Lydenburg, Makahane and Graskop was studied. Normal dispersive Raman spectroscopy was found to be the most effective analytical technique in this study. XRF, XRD and FT-IR spectroscopy were used as complementary techniques. All representative samples contained common features, which were characterised by kaolin ($Al_2Si_2O_5(OH)_5$), illite ($KAl_4(Si_7AlO_{20})(OH)_4$), feldspar (K- and $NaAlSi_3O_8$), quartz (α-SiO_2), hematite (α-Fe_2O_3), montmorillonite ($Mg_3(Si,Al)_4(OH)_2{\cdot}4.5H_2O[Mg]_{0.35}$), and calcium silicate ($CaSiO_3$). Gypsum ($CaSO_4{\cdot}2H_2O$) and calcium carbonates (most likely calcite, $CaCO_3$) were detected by Raman spectroscopy in Lydenburg, Makahane and Graskop shards. Amorphous carbon (with accompanying phosphates) was observed in the Raman spectra of Lydenburg, Rooiwal and Makahane shards, while rutile (TiO_2) appeared only in Makahane shard. The Raman spectra of Lydenburg and Rooiwal shards further showed the presence of anhydrite ($CaSO_4$). The results showed that South African potters used a mixture of clays as raw materials. The firing temperature for most samples did not exceed 800 °C, which suggests the use of open fire. The reddish brown and grayish black colours were likely due to hematite and amorphous carbon, respectively.

Keywords: South African; Pottery; Raman; Kaolin; Illite

1. Introduction

The technique of Raman spectroscopy was used to examine a series of African domestic clay pottery shards. Such a detailed examination of pottery could give valuable information on the characterisation of archaeological items by the identification of materials such as pigments, binders and clays used in the manufacturing process. The importance of this subject has already been demonstrated in the literature [1–3]. The chemical composition can be used to define the pottery of a particular area and people by determining the raw materials used. For very important artefacts the knowledge of the composition of raw materials and processing methods used will help in the reconstruction of such pieces. For instance, studies have shown that natural sources of Ca^{2+} in clay may be ash, bedrock clay bodies, shells (containing Ca particles), etc. while sources of P_2O_5 in clays are dung, blood, fats and lipids [4]. The bushmen are known to anoint their clay vessels with fat while still damp, then to smear them with gum after drying and to boil springbok blood in them after they were fired. The protein-based stem extraction product from animal bones and butcher's offal which is normally referred to as animal glue is a nitrogen-containing material. Animal glue is usually applied to pottery before colouring with metal-containing pigments [5].

There are two ways in which the pottery could be fired: in an open fire and in a kiln. The open firing methods have an upper limit of 800 °C [4]. The kilns were used for iron smelting and could reach a maximum temperature of 1230 °C.

Various techniques have been used to analyse pottery for defining non-local pottery; neutron activation, X-ray diffractometry (XRD), trace elemental analysis, spectroscopy, etc. by chemically and mineralogically characterising the clay paste [6]. However, the paste analysis is complicated by the diversity of clay minerals and trace elements in nature. Chemical analysis is applied in clay pottery for characterisation, as different clay deposits can be distinguished by their chemical composition. Optical emission spectroscopy is used for analysis of minor and/or trace elements [7]. The success of these approaches is

* Corresponding author. Tel.: +27 124203099; fax: +27 123625297.
E-mail address: danita.dewaal@up.ac.za (D. de Waal).

1386-1425/$ – see front matter © 2006 Elsevier B.V. All rights reserved.
doi:10.1016/j.saa.2006.02.059

constrained by data on regional and interregional distribution of clays and trace elements. Tempering (aplastic) agents in the pottery are often well suited for use as indicators of provenance and origin, even though they could be traded. The aplastics are often used to retain the shape of the pottery controlling the shrinkage during drying and firing [6]. Many tempering agents are not good indicators of source area, e.g. bone and shells, because they are common, but rock fragments and sand grain are better due to the fact that they may reflect geological source.

In this paper, we report on the results obtained by Raman spectroscopy during the determination of the main components of selected South African earthenware (low temperature fired clay pottery) objects in the form of domestic clay pottery shards. The purpose of the study was to characterise the samples on the basis of their chemical composition as obtained from their Raman spectra. This will help determine whether the same raw materials were used, and if so, whether the pottery samples were processed under the same conditions. It is intended that these results will help in revealing the potential of Raman spectroscopy as a tool in analysing earthenware pottery shards and their methods of production in South Africa.

2. Experimental

2.1. Samples

The samples originate from four areas in South Africa, namely, Lydenburg (Fig. 1), Makahane (Fig. 2), Graskop (Fig. 3) and Rooiwal (Fig. 4). The Makahane collection was obtained from an archaeological site just outside the Kruger National Park. The shards were found at the same location back in the 1930s. These were dated back to the 13th and 14th century, and most likely belonged to the Venda- and Pedi-speaking people who lived in that region. The Graskop collection was found at a place presently known as the Aventura Resort. Samples 1–6 were found in the Aventura Resort cave, while 7 and 8 were outside the cave, but in the vicinity. These have been dated to the 13th century. The people believed to have resided in the Aventura caves are the Swazi-speaking people. The Lydenburg collection, even though obtained from the same area, was not necessarily found at the same location. The date of these shards is the 14th century. The single shard, which was not dated was found in an area called Rooiwal, in Gauteng province, Republic of South Africa. The Graskop, Lydenburg and Makahane sites are situated within 40 km of each other in Mpumalanga province near the border of South Africa and Swaziland.

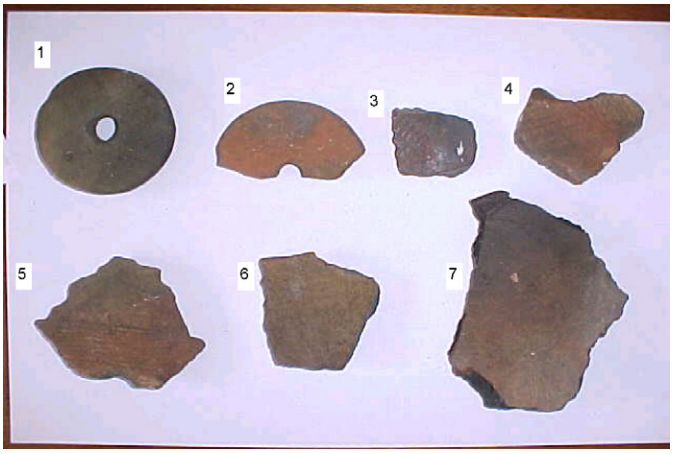

Fig. 2. Makahane shards: (1) black (no decorations); (2) orange-red surface and gray body with line (short and long) impressions; (3) orange-red outside and dark-brown inside (crossing line impressions); (4) orange-red with gray patches (with array of short line impressions); (5) reddish brown on one side and dark-brown on the other (with crooked line impressions); (6) yellowish brown on one side and reddish brown on the other (with short line impressions); (7) reddish brown and black on other areas (with short line impressions). (For interpretation of the references to color in this figure legend, the reader is referred to the web version of the article.)

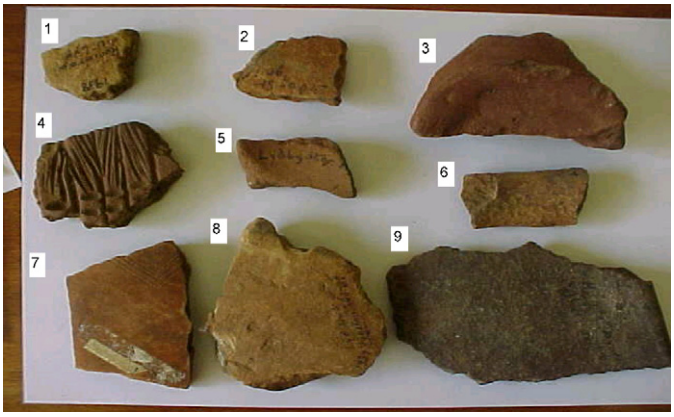

Fig. 1. Lydenburg shards: (1) dark red with impressions; (2) yellowish red with line impressions; (3) dark red with shape of pottery bottom (no decorations); (4) yellowish red with deep line impressions; (5) reddish brown with deep line impressions; (6) reddish brown with short parallel lines; (7) dark red with line impressions; (8) yellowish brown (no decorations); (9) reddish black (no decorations). (For interpretation of the references to color in this figure legend, the reader is referred to the web version of the article.)

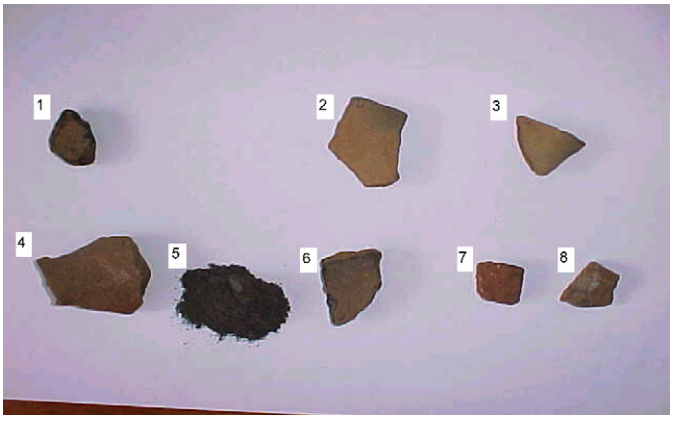

Fig. 3. Graskop shards: (1) light brown but black under surface (no decorations); (2) yellowish brown (no decorations); (3) yellowish brown (no decorations); (4) dark brown with deep line impressions; (5) light brown but black under surface (no decorations, but crushed); (6) light brown surface but black under surface (with short line decorations); (7) orange red with zig-zag impressions; (8) light brown with deep straight line impressions. (For interpretation of the references to color in this figure legend, the reader is referred to the web version of the article.)

Fig. 4. Rooiwal shard. Dark-brown on the outside and black burnt material in the inside. (For interpretation of the references to color in this figure legend, the reader is referred to the web version of the article.)

2.2. Instruments

2.2.1. Raman spectroscopy

Laser Raman spectra were collected at room temperature using a Dilor XY Raman spectrometer with a resolution of 2 cm^{-1}. Radiation at 514.5 nm from an Ar^+ Coherent Innova 300 laser was used to excite the samples. The laser power was set at 100 mW at the source. The recording time was set at between 30 and 180 s, with two accumulations per spectrum segment. An Olympus Mplan 100× objective on an Olympus BH-2 microscope was used to focus on the sample. The Raman spectra were analysed using Labspec v 2.04 software [8].

2.2.2. X-ray powder diffractometry

The X-ray diffraction (XRD) analyses were performed using a Cu Kα (1.5418 Å) source (40 kV, 40 mA) from a Siemens D-501, with a graphite secondary monochromator and a scintillation counter detector. The powdered sample was placed on a flat plastic plate, which was rotated at 30 rpm. The scans were performed at 25 °C in steps of 0.04°, with a recording time of 2 s for each step [9]. Where accurate 2θ values were required, Si was added as internal 2θ standard.

2.2.3. Infrared spectroscopy

The infrared spectra were recorded in the mid-infrared region (400–4000 cm^{-1}) in an evacuated chamber of Bruker 113v FT-IR spectrometer using KBr discs as matrices. A spectral resolution of 2 cm^{-1} was used and spectra were accumulated over 32 scans. The FT-IR spectroscopy was applied to all samples. Only 2 mg of each sample was mixed with 100 mg of KBr and pressed under 6 tonnes for 2 min in making the disk. At first (for Makahane sample no. 7, Graskop sample no. 5, Lydenburg sample no. 8 and Rooiwal sample) the samples were crushed and ground before making the KBr pellets.

The fitting of peaks and smoothing were done with OPUS 2000 software on the Bruker 113v over the working window, 400–4000 cm^{-1}.

2.2.4. X-ray fluorescence

An ARL 9400XP+ Wavelength-dispersive XRF Spectrometer with a Rh source was used for the X-ray fluorescence analyses of the samples. The XRF Spectrometer was calibrated with certified reference materials. The NBSGSC fundamental parameter program was used for matrix correction of major elements, as well as Cl, Co, Cr, V, Sc and S. The Rh Compton peak ratio method was used for the other trace elements. Samples were dried and fired at 1000 °C to determine the percentage loss on ignition; for the samples this was less than 2%. Major element analyses were carried out on fused beads, following the standard method used in the XRD and XRF laboratory of the University of Pretoria [10], as adapted from Bennett and Oliver [11]. A prefired sample of 1 and 6 g of lithium tetraborate flux was mixed in a 5% Au/Pt crucible and fused at 1000 °C in a muffle furnace, with occasional swirling. The glass disk was transferred into a preheated Pt/Au mould and the bottom surface was analysed. The trace element analyses were done on pressed powder pellets, using an adaptation of the method described by Watson [12], with a saturated Mowiol 40–88 solution as binder.

3. Results and discussion

The representative shards were Lydenburg sample no. 8, Makahane sample no. 7, Graskop sample no. 5 and the Rooiwal sample. The laser was focused in each recording on coloured areas visible on the object under the microscope. The predominant colours on the shards were black, orange, red and maroon scattered over the uncoloured background. This is normally an indication of the composite nature of clay products. A range of spectra was collected from different spots on each sample. The regions with similar colours (e.g. black) were not homogeneous and did not necessarily give similar spectra and composition. The spectra obtained for all samples were characterised mainly by the presence of aluminosilicates, inorganic phases and pigments [13,14].

All Raman bands together with their assignments obtained from various coloured areas on all representative samples are presented in Table 1. Typical Raman spectra of all samples recorded under microscopic conditions are shown in Figs. 5–8

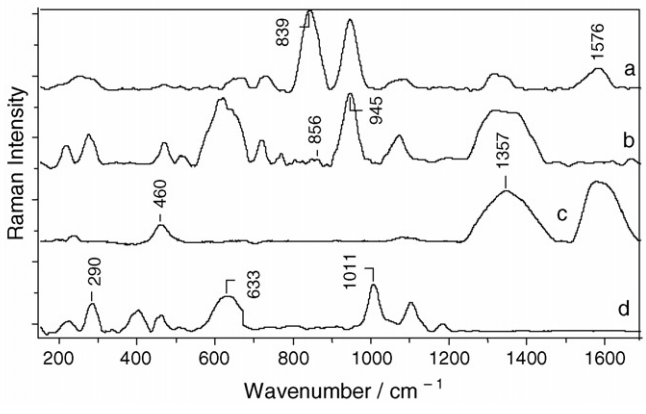

Fig. 5. Raman spectra obtained from Lydenburg shard no. 8.

Table 1
The Raman assignments of phases in the South African clay pottery

A Raman (cm^{-1})	B Raman (cm^{-1})	C Raman (cm^{-1})	D Raman (cm^{-1})	E	F	I
1576	1599		1605	Am. C[a]	C–C str	[41–43]
1358	1353		1349	Am. C	C–C str	[41–43]
1185			1175	Anhydrite	S–O str	[20,44]
1123			1125	Anhydrite	S–O str	[20,44]
1087	1082	1089		CO_3^{2-}	C–O str	[20,31,34,35]
1071	1055	1057		$CaSiO_3$	Si–O str	[13,46,45]
1011		1003		Gypsum	S–O str	[20,31,35]
	983	983		Feldspar	Si–O str	[26]
972	976			PO_4^{3-}	P–O str	[13,35]
			915	Montmor[b]	AlOH bend	[30]
856	895	863	860	$CaSiO_3$	Si–O str	[30,46]
839	821	809	836	Montmor	AlOH bend	[30]
771		793		Illite	Al–O–Si bend	[29]
729	760	746	759	CO_3^{2-}/kaolin	C–O/O–H bend	[19,31]
716	710	707	709	Illite	Al–O bend	[29]
680	685	689/671		Gypsum	S–O bend	[20,31,35]
660	660	665	650/667	Kaolin	Al–O–Si bend	[19]
633			627	Kaolin	Al–O str	[19]
	617			Rutile	Ti–O str	[20]
612		601	608	Hematite	Fe–O str	[14,16,17,20]
		538	556	Kaolin	Si–O–Al bend	[19]
509/520	511	511	504	Feldspar	Al–O–Si bend	[39]
472				Kaolin	Al–O–Si bend	[19]
460	461	464	464	Quartz/illite	Si–O–Si bend	[13,17,18,29]
	434			Rutile	Ti–O bend	[20]
405	402	403		Hematite	Fe–O bend	[14,17,20]
		400		$Ca_3(PO_4)_2$	P–O bend	[13]
	369	376	378	Quartz	Si–O bend	[18]
	333	324	358	Kaolin	O–H–O bend	[19]
290	285	288	280	Kaolin/hematite	O–H–O, Fe–O bend	[17–19]
275	278	276	278	CO_3^{2-}	C–O bend	[20,31]
246				Quartz	Si–O bend	[18]
235				Kaolin	O–H–O bend	[19]
218	222	222	220	Hematite	Fe–O bend	[20]
201			204	Kaolin	O–H–O bend	[19]

The wavenumbers are a summary of spectra obtained on all different shards in a particular collection. A, Lydenburg sample no. 8; B, Makahane sample no. 7; C, Graskop sample no. 5; D, Rooiwal sample; E, chemical phase; F, assignment; I, references.

[a] Amorphous carbon.

[b] Montmorillonite.

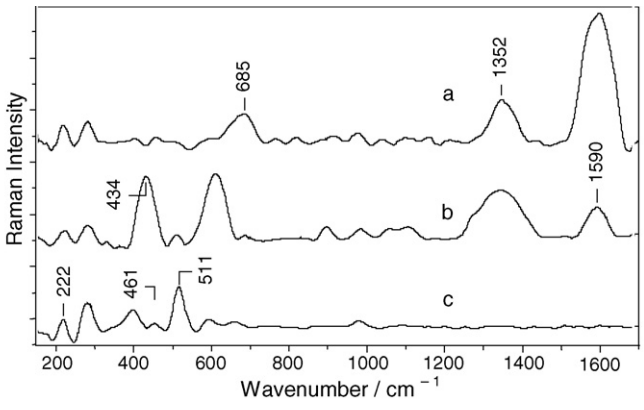

Fig. 6. Raman spectra obtained from Makahane shard no. 7.

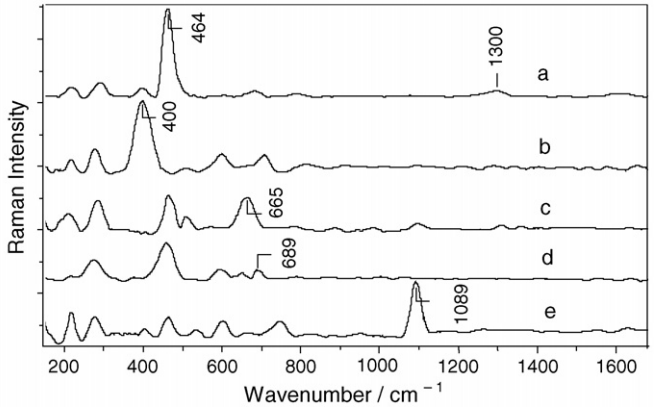

Fig. 7. Raman spectra obtained from Graskop shard no. 5.

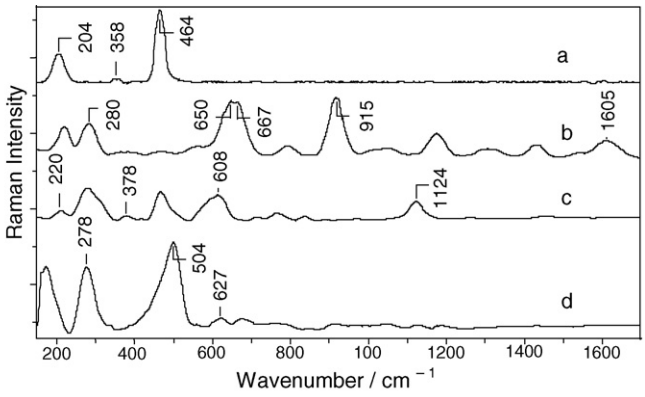

Fig. 8. Raman spectra obtained from Rooiwal shard.

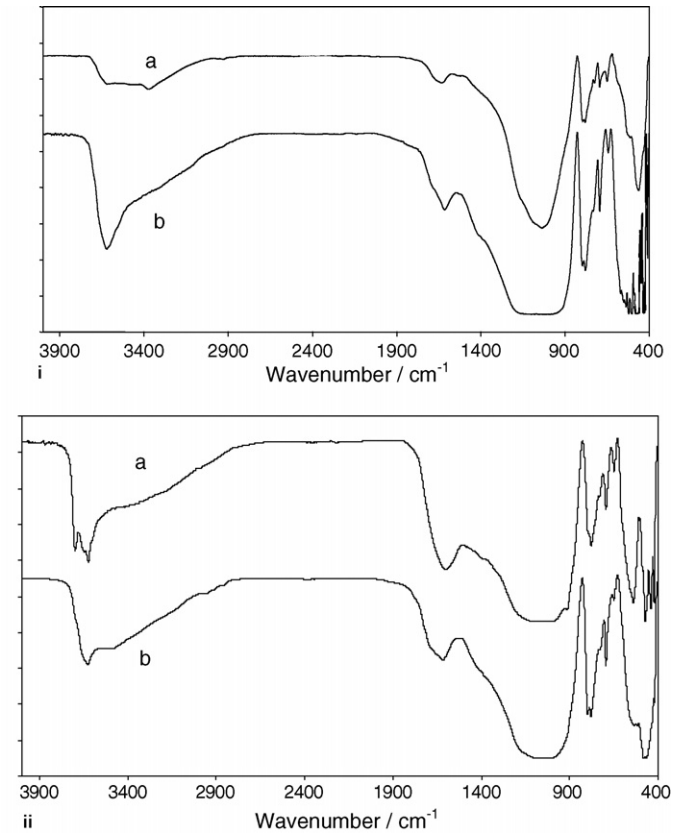

Fig. 9. (i) (a) FT-IR spectrum obtained from Makahane shard and (b) FT-IR spectrum obtained from Graskop shard. (ii) (a) FT-IR spectrum obtained from Rooiwal shard and (b) FT-IR spectrum obtained from Lydenburg shard.

for the wavenumber range 150–1700 cm^{-1}. The chemical phases detected by Raman spectroscopy in all representative samples include hematite, quartz, feldspar, kaolin, montmorillonite, illite and calcium silicate. Other phases observed in some samples are rutile, gypsum, phosphate, calcium carbonate, anhydrite, calcium silicate and amorphous carbon.

The bands around 220, 280 and 405 cm^{-1} are due to red iron(III) oxide [15–20], see Figs. 5 and 6 and Table 1. Due to the presence of the reddish areas throughout the sample and in the bulk of the body, this pigment could have been part of the starting material [21]. It also could have been added as a red pigment or in some other form, e.g. Fe_3O_4, $Fe(OH)_3$, etc., occurring naturally in clay [14,22], that was in turn converted into hematite, α-Fe_2O_3. The clay bodies and pastes used by African potters are normally brownish gray [22] in colour and various colours only develop during the process (particularly during firing). The reddish brown colour of most of the shards is due to relatively high iron oxide (α-Fe_2O_3) content. The XRF results show that the content of hematite (α-Fe_2O_3) is relatively high, $\geq$7 mass%. It has been reported that hematite is one of the most intense colouring materials. Only 1–1.5 mass% of hematite is required to give soil a reddish colour [23]. The presence of this compound is confirmed by XRD results.

The strongest Raman bands appearing around 460 cm^{-1} are due to quartz (see Figs. 7 and 8). The sandstones are most probably the natural source of quartz in this sample. These bands are normally very intense and narrow when quartz is in its free and isolated form, SiO_2 [18,13]. The presence of this band in its broadened form could be due to the slightly distorted crystal structure of quartz as it undergoes transformation during processing. Illite clay mineral also shows an intense band in the vicinity of 460 cm^{-1} and its presence will cause band overlap.

The strong intensity of the band around 460 cm^{-1} (in the Lydenburg, Graskop and Rooiwal shards) suggests high content of quartz. The FT-IR results (Fig. 9 and Table 2) also show intense absorption peaks normally associated with quartz (779 and 797 cm^{-1}) [24(a),25(a)].

The XRF and XRD results also suggest higher percentage of the quartz phase (Tables 3 and 4). The low intensity of this band (in the Makahane shard) may be an indication of the fused form of the quartz phase [18] or the breakdown in the skeletal structure of quartz as it reacts to form new phases.

The Raman spectroscopic analysis of all samples also shows the presence of kaolin clay mineral, indicated by the bands around 660 cm^{-1} [17–19]. The appearance of kaolin in the finished product suggests that the processing temperature was not high enough (i.e. $\leq$800 °C) to effect complete dissolution of this clay mineral [26]. The firing of African pottery is normally done in an open fire that reaches temperatures of around 800 °C [4]. The presence of kaolin is further confirmed by the FT-IR and XRD results (Tables 2 and 4, respectively).

Natural clay minerals often occur as mixtures [27,28]. In all samples, Raman spectroscopy showed features resembling those of illite clay mineral. The features associated with illite appear around 707 and 781 cm^{-1} [29–30]. The broad and intense band around 460 cm^{-1} could be due to the overlapping of the quartz and illite bands. The bands around 810 and 830 cm^{-1} in all representative samples are normally associated with those of montmorillonite clay mineral [30,32]. The presence of both clay minerals confirms that the firing temperatures were below 850 °C, because the skeletal structure of both illite and montmorillonite begin to break down around 850 °C [33]. FT-IR spectroscopy confirms the presence of illite and montmorillonite. The absorption bands of illite appear around 752 and 3620 cm^{-1} and that for montmorillonite around 3620 cm^{-1} (see Fig. 9(i) and Table 2).

Table 2
The IR assignments of phases in the South African clay pottery

A IR (cm^{-1})	B IR (cm^{-1})	C IR (cm^{-1})	D IR (cm^{-1})	E	F [17,19,24,48]
		3697		Kaolin	O–H str
		3654		Kaolin	O–H str
3626	3624	3624	3622	Kaolin/illite/Montmor[a]	O–H str
3429	3423	3410		Water	O–H str
1617	1622	1629	1629	Water	H–O–H bend
1080	1080	1096	1087	Amorph. Al–Si[b]	Al–O–Si str
1034	1036	1034	1035	Kaolin	Si–O–Si str
915		914	914	Kaolin	Al–O–H str
837		850	845	Illite/montmor	Al–O–H str
798	795	796	797	Quartz/kaolinite	Si–O bend
778	779	778	779	Quartz	Si–O–Si str
750	750	750	752	Illite	Al–O–Si bend
723	724	727	724	Feldspar/CO_3^{2-}	Al–O–Si str/C–O bend
695	695	694	695	Quartz/CO_3^{2-}	Si–O bend/C–O bend
652	650	645	648	Feldspar	Al–O–Si str
538	529	530	530	Kaolin/hematite	Al–O–Si/Fe–O bend
475	484	470	476	Kaolin/hematite	O–Si–O/Fe–O bend
	435	434		Kaolin	O–Si–O bend

The wavenumbers are a summary of spectra obtained for all different shards in a particular collection. A, Lydenburg sample no. 8; B, Makahane sample no. 7; C, Graskop sample no. 5; D, Rooiwal sample; E, chemical phase; F, assignment.
[a] Montmorillonite.
[b] Amorphous aluminosilicates.

Table 3
The XRF results of Graskop sample no. 5, Makahane sample no. 7, Lydenburg sample no. 8 and Rooiwal sample, given as normalised % concentration

Sample	SiO_2	Al_2O_3	Fe_2O_3	CaO	K_2O	TiO_2	MgO	P_2O_5	SO_3	Total
Graskop	51.9	28.3	13.9	0.72	2.42	1.00	0.18	0.14	0.14	98.70
Makahane	57.7	20.4	12.3	2.29	2.17	1.99	1.46	1.46	–	99.77
Lydenburg	64.0	23.8	6.93	0.92	0.99	1.56	0.88	0.007	0.253	99.34
Rooiwal	57.3	18.5	8.46	2.65	8.79	0.62	1.41	1.18	0.171	99.08

Note that heavy metals and other metals at low concentrations also occur but are not shown in this table.

The Raman spectra of all samples, except Rooiwal shard, further showed prominent features around 278 and 1087 cm^{-1}. These bands have previously been associated with calcite ($CaCO_3$) [18–20,31,34,35]. The presence of this phase further confirms the processing temperatures below 800 °C [36]. The natural sources of calcite include shells and limestone [36]. This means calcite occurs as an impurity in clays [22,37]. The XRF results suggest small amounts of calcite, below 1 mass%. Some calcite appears to have reacted with aluminosilicates to form feldspar, $(NaCa)Al(Si,Al)_3O_8$, as indicated by the XRD results. The pure calcium carbonate could not be detected by XRD, perhaps due to its low content or poor crystallinity [26]. It has been reported that calcium carbonate obtained from calcareous weathering crusts is non-crystalline [38(a)]. The FT-IR spectrum shows weak features previously associated with non-crystalline calcium carbonate at 695 and 724 cm^{-1} [24(b)].

Table 4
The XRD results on Graskop sample no. 5, Makahane sample no. 7, Lydenburg sample no. 8 and Rooiwal sample

Sample	Quartz	Feldspar	Kaolinite	Illite	Hematite
Graskop	√	√	√	√	√
Makahane	√	√	√	×	√
Lydenburg	√	√	√	√	√
Rooiwal	√	√	√	√	√

The presence of feldspar (albite) in all samples is shown by the Raman bands around 511 cm^{-1} [39], see Fig. 5 and Table 1. Absorption bands around 648 and 724 cm^{-1} manifest this phase. The identity of this feldspar is confirmed by XRD results, which further show the presence of another feldspar phase, microcline, Table 4. Albite and microcline are both known as alkali feldspar, Na and K end-member compositions, respectively, and have similar occurrence in rocks, such as granite, rhyolite, etc. [24(c),24(d)].

The intense broad bands around 1358 and 1576 cm^{-1} in the Lydenburg and Makahane shards suggest the presence of amorphous carbon [40–43]. The amorphous carbon is most likely bone black because of the corresponding peak around 970 cm^{-1}. When the bone collagen is calcined the organic matter results in carbon, while the inorganic matter forms phosphates. Therefore, the band occurring around 970 cm^{-1} is likely due to the phosphate ions [20]. The XRF results show very low content of phosphorus (Table 3) and no phosphorus compound could be detected by XRD analysis. The FT-IR spectrum showed no bands associated with phosphates perhaps due to their low con-

tent. The 1358 and 1576 cm^{-1} bands are assigned to the sp^3 and sp^2 bands of hybridised carbon [40–43], respectively, the so-called D and G bands. The ratio of intensities of these bands indicates the graphitic content of the amorphous carbon. From the relative intensities of these bands the sp^2 (G band) appear to be slightly stronger, suggesting more graphitic nature of the amorphous carbon for the Lydenburg shard. However, Fig. 5(b) shows only the D band, suggesting very low graphitic nature. It is difficult to conclude on the graphitic nature of the amorphous carbon in Makahane shard because the relative intensities of the D and G bands do not seem to follow any identifiable trend.

The Raman bands appearing around 1125 and 1175 cm^{-1} strongly suggest the presence of anhydrite ($CaSO_4$) [20,44] in Lydenburg and Rooiwal shards. This component could either have been part of the clay minerals or developed during the processing, e.g. from the dehydration of gypsum ($CaSO_4{\cdot}2H_2O$). The residual SO_3 detected by XRF may be due to oxidation of sulphur-containing compounds during firing. The XRD analysis expectedly showed no anhydrite because of its low content in the sample. Anhydrite is found as a massive rock of large extension and often occurs in natural clays [25(b)].

The Raman band that occurs around 617 cm^{-1} in the spectra of Makahane shard is characteristic of rutile (α-TiO_2) [18,20]. The relative amount of this phase as obtained from the XRF results is found to be ~2 mass%. However, it could not be detected by XRD analysis. The reason for this could be its low content or poor crystallinity. The titanium dioxide absorption spectrum shows very broad and weak bands in the region 400–1600 cm^{-1} [25(c)]. The presence of this phase suggests that the firing temperatures for Lydenburg and Makahane shards could have slightly exceeded 800 °C [18].

The presence of $CaSiO_3$ is suggested by the appearance of Raman bands around 860 and 1055 cm^{-1} [18,13,45,46] in all samples. Clays with high calcium carbonate content can form compact ceramic structures at lower firing temperatures because of the reactivity of carbonate. It easily reacts with quartz and other clay minerals to form $CaSiO_3$ [18,13]. The reaction of $CaCO_3$ often occurs at temperatures above 800 °C [36,47]. The $CaSiO_3$ phase is built of isolated $Si_3O_9^{6-}$ units between Ca^{2+} ions [18]. It is commonly associated with glassy aluminosilicates, even though it could occur in crystalline form. The presence of this phase suggests that the processing conditions were such that the carbonates were beginning to decompose into CaO and CO_2 most likely between 600 and 800 °C [26,47].

The Raman bands around 680 and 1007 cm^{-1} observed for Lydenburg, Makahane and Graskop shards are characteristic of gypsum ($CaSO_4{\cdot}2H_2O$) [20,35,36,46,48]. Gypsum is a common mineral widely distributed in sedimentary rocks and it frequently occurs interstratified with limestone and shales [38(b)].

The Raman spectrum (Fig. 7(b)) of the Graskop shard shows a distinct intense band around 400 cm^{-1}. This band occurs in the region for the E_g vibration mode of hematite. However, its strong intensity relative to the bands around 220 and 280 cm^{-1} makes its assignment uncertain. Table 5 gives a summary of all the chemical phases identified by Raman spectroscopy in all representative samples.

Table 5
The chemical phases identified by Raman spectroscopy in each representative sample

Compound	Lydenburg	Makahane	Graskop	Rooiwal
Kaolin	√	√	√	√
Hematite	√	√	√	√
Quartz	√	√	√	√
Feldspar	√	√	√	√
Carbonates	√	√	√	×
Montmorillonite	√	√	√	√
Illite	√	√	√	√
Gypsum	√	√	√	×
Anhydrite	√	×	×	√
$CaSiO_3$	√	√	√	√
Amorph. carbon	√	√	×	√
Phosphates	√	√	×	×
Rutile	×	√	×	×

4. Conclusion

Raman spectroscopy has been successfully used to determine the composition of African clay pottery shards from a selected number of South African archaeological sites (Lydenburg, Makahane, Graskop and Rooiwal). Despite the low Raman scattering effects of clay components and fluorescence commonly associated with this type of samples, important results were obtained in this study. A total of 13 chemical phases were identified by Raman spectroscopy in the samples investigated. The identification of so many chemical components in the low temperature fired clay products demonstrates the high sensitivity and applicability of Raman spectroscopy to these type of samples.

All representative shards (Lydenburg sample no. 8, Makahane sample no. 7, Graskop sample no. 5 and Rooiwal sample) from the four locations contained common features, which are characterised by kaolin, illite, quartz, feldspar, hematite, montmorillonite and $CaSiO_3$. The reason for this could be that the clay minerals and pottery making process did not vary significantly in the region that included the locations from which the samples were obtained. The potters could also have used common clay quarries.

The results confirmed that the samples under investigation were fired at lower temperatures, as indicated by the presence of clay minerals (kaolin, montmorillonite and illite). A minimum of two clay minerals was observed in each sample, which proves that the clay minerals in the locations investigated occur as mixtures. The presence of calcium carbonate in Lydenburg, Makahane and Graskop shards suggests that the pottery from which the shards were derived were fired at temperatures below 800 °C. The Makahane shard further shows the presence of rutile. This compound has been reported as a high temperature phase, which is formed between 800 and 1100 °C. The raw materials could also have been mixed with TiO_2 in rutile form. Therefore, it is likely that the firing temperature for Makahane shard reached some value above 800 °C. The pottery could have been fired at that high temperature for a short time, thus preserving the structures of calcium carbonate and clay minerals.

The compounds that gave the samples reddish brown and black colours are hematite and amorphous carbon, respectively.

Other compounds, which were observed in various samples, either occurred as impurities in the clay minerals (e.g. gypsum) or were formed during the firing process (e.g. anhydrite, calcium silicate and phosphates).

For the samples analysed, the results further showed that there is an overlapping of components between the sites and that no chemical species was unique to any one particular site. Due to its ability to detect various chemical species in low temperature fired clay products (as shown in this study), Raman spectroscopy can be useful in determining the raw materials used, processing conditions and discrimination based on unique chemical compounds.

Acknowledgements

The financial support by the National Research Foundation in Pretoria and the University of Pretoria is gratefully acknowledged. The authors would also like to thank Annette Weitz from the Centre for Indigenous studies for the supply of samples and historical information.

References

[1] J. Poblome, P. Degryse, W. Viaene, R. Ottenburgs, M. Waelkans, R. Degeest, J. Noud, J. Archaeol. Sci. 29 (2002) 873.
[2] R.J.H. Clark, Chem. Soc. Rev. 24 (1995) 187.
[3] R. Davey, D.J. Gardiner, B.W. Singer, M. Spoke, J. Raman Spectrosc. 25 (1994) 53.
[4] C.A. Bollang, J.C. Vogel, L. Jacobson, W.A. van der Westhuizen, C.G. Sampson, J. Archaeol. Sci. 20 (1983) 41.
[5] G.V. Robins, C. del Re, N.J. Sedey, A.G. Davis, J.A.A. Hawari, J. Archaeol. Sci. 10 (1983) 385.
[6] C.R. Ferring, T.K. Perttula, J. Archaeol. Sci. 14 (1987) 437.
[7] P.S. Peacock, J. Archaeol. Sci. 3 (1976) 271.
[8] Labspec, version 2.04, Distributed by Dilor SA & Universite' de Reims, France, 1997.
[9] S. Verryn, Details of XRD Procedure Used at the University of Pretoria, XRD Laboratory, Personal Written Communication, University of Pretoria, Pretoria, 2002.
[10] M. L. Loubser, (Typed) Report on XRF Analyses of Ceramics. mloubser@postino.up.ac.za, June 20, 2002.
[11] H. Bennet, G. Oliver, XRF Analysis of Ceramics, Minerals and Applied Materials Wiley, Chichester, 1997, p. 37.
[12] J.S. Watson, X-ray Spectrum 25 (1996) 173.
[13] P. Colomban, F. Treppoz, J. Raman Spectrosc. 32 (2001) 93.
[14] J. Zuo, C. Xu, C. Wang, Z. Yushi, J. Raman Spectrosc. 30 (1999) 1053.
[15] H.G.M. Edwards, C.J. Brooke, J.K.F. Tait, J. Raman Spectrosc. 28 (1997) 95.
[16] D. Crossley, Post-Medieval Archaeology in Britain, Leicester University Press, Leicester, 1990, p. 188.
[17] D. Bikiaris, S. Daniila, S. Sotiropoulou, O. Katsimbiri, E. Poulidou, P. Moutsatsou, Y. Chryssoulakis, Spectrochim. Acta Part A 56 (1999) 3.
[18] N.Q. Liem, G. Sagon, V.X. Quang, H. Van Tan, P. Colomban, J. Raman Spectrosc. 31 (2000) 933.
[19] R.L. Frost, P.M. Fredericks, J.R. Bartlett, Spectrochim. Acta Part A 49 (1993) 667.
[20] H.G.M. Edwards, E.M. Newton, J. Russ, J. Mol. Str. 550–551 (2000) 245.
[21] D. Hradil, T. Grygar, J. Hradilova, P. Bezdička, Appl. Clay Sci. 22 (2003) 223.
[22] G.W.A. Nyakairu, H. Kurzwell, C. Koeberl, J. Afri. Earth Sci. 35 (2000) 123.
[23] U. Schwertmann, in: J.M. Bigham, E.J. Ciolkosz (Eds.), Soil Color, vol. 31, Soil Science Society of American Special Publication, Madison, Wiscons, 1993, p. 51.
[24] (a) M.J. Wilson, Clay Mineralogy: Spectroscopic and Chemical Determinative Methods, Chapman and Hall, London, 1994, p. 52;
(b) M.J. Wilson, Clay Mineralogy: Spectroscopic and Chemical Determinative Methods, Chapman and Hall, London, 1994, p. 55;
(c) M.J. Wilson, Clay Mineralogy: Spectroscopic and Chemical Determinative Methods, Chapman and Hall, London, 1994, p. 33;
(d) M.J. Wilson, Clay Mineralogy: Spectroscopic and Chemical Determinative Methods, Chapman & Hall, London, 1994, p. 34.
[25] (a) H.W. van der Marel, H. Beutelspacher, Atlas of Infrared Spectroscopy of Clay Minerals and their Admixtures, Elsevier Scientific Publishing Company, Amsterdam, Oxford, New York, 1976, p. 234;
(b) H.W. van der Marel, H. Beutelspacher, Atlas of Infrared Spectroscopy of Clay Minerals and their Admixtures, Elsevier Scientific Publishing Company, Amsterdam, Oxford, New York, 1976, p. 249;
(c) H.W. van der Marel, H. Beutelspacher, Atlas of Infrared Spectroscopy of Clay Minerals and their Admixtures, Elsevier Scientific Publishing Company, Amsterdam, Oxford, New York, 1976, p. 259.
[26] J.M. Alia, H.G.M. Edwards, F.J. Garcia-Navaro, J. Parras-Armenteros, C.J. Sanchez-Jimenez, Talanta 50 (1999) 291.
[27] L. Jankovič, P. Komadel, J. Catal. 218 (2003) 227.
[28] F. Kooli, W. Jones, Clay Miner. 32 (1997) 633.
[29] W. Liu, Water Res. 35 (2001) 4111.
[30] R.L. Frost, L. Rintoul, Appl. Clay Sci. 11 (1996) 171.
[31] V.C. Farmer, in: H. Van Olphen, J.J. Fripiat (Eds.), Data Handbook for Clay Minerals and Other Non-metallic Minerals, Pergamon, Oxford, 1979, p. 307.
[32] R.L. Frost, J.T. Kloprogge, Spectrochim. Acta Part A 56 (2000) 2177.
[33] E. Ingerson, in: F. Bruce, Bohor (Eds.), High Temperature Phase Development in Illitic Clays, Proceedings of the 12th National Conference, Monograph No. 19, Pergamon, New York, 1971, p. 233.
[34] E.E. Coleyshaw, W.P. Griffith, R.J. Bowell, Spectrochim. Acta Part A 50 (1994) 1909.
[35] I.A. Degen, G.A. Newman, Spectrochim. Acta Part A 49 (1993) 859.
[36] M.M. Jordan, T. Sanfeliu, C. de la Fuente, Appl. Clay Sci. 20 (2001) 87.
[37] P. Valfre, Yixing Teapots for Europe, Edition Exotic Line, Janvier, China, 2000, p. 387.
[38] (a) C.S. Hurlbut Jr., C. Klein, Manual of Mineraology, 19th ed., John Wiley and Sons Inc., New York, 1971, p. 431;
(b) C.S. Hurlbut Jr., C. Klein, Manual of Mineraology, 19th ed., John Wiley and Sons Inc., New York, 1971, p. 322.
[39] R. Gout, E.H. Oelkers, J. Schott, A. Zwick, Geochim. Cosmochim. Acta 61 (1997) 3013.
[40] M. Tabbal, T. Christidis, S. Isber, M.A. El Khakani, P. Merel, M. Chaker, Thin Solid Films 453–454 (2004) 234.
[41] R.N. Tarrant, D.R. McKenzie, M.M.M. Bilek, Diamond Relat. Mater. 13 (2004) 1422.
[42] K. Lee, H. Sugimura, Y. Inoue, O. Takai, Diamond Relat. Mater. 13 (2004) 507.
[43] J.C. Orlianges, C. Champeaux, A. Catherinot, Th. Merle, B. Angleraud, Thin Solid Films 453–454 (2004) 285.
[44] C.H. Chio, S.K. Sharma, D.W. Muenow, Am. Miner. 89 (2004) 390.
[45] B. Mihailova, E. Dinolova, L. Konstantinov, J. Non-Crystal. Solids 191 (1995) 79.
[46] C.D. Yin, M. Okuno, H. Morikawa, F. Marumo, T. Yamanaka, J. Non-Crystal. Solids 80 (1986) 167.
[47] J.V. Owen, J. Archaeol. Sci. 24 (1997) 301.
[48] R.R. Shagidullin, A.V. Chernova, V.S. Vinogradova, F.S. Mukhametov, Atlas of IR Spectra of Organophosphorus Compounds (Interpreted Spectrograms), Kluwer Academic Publishers, Boston, 1990, p. 14.